
This is the **submitted version** of the book part:

Leuermann, Jonas; Fernandez-Gavela, Adrian; Halir, Robert; [et al.]. «Silicon photonic label free biosensors with coherent readout». A: 2020 22nd International Conference on Transparent Optical Networks (ICTON). 2020. DOI 10.1109/ICTON51198.2020.9203519

This version is available at <https://ddd.uab.cat/record/236011>

under the terms of the  IN COPYRIGHT license

Silicon photonic label free biosensors with coherent readout

Jonas Leuermann^{1,2}, Adrián Fernández-Gavela³, Robert Halir^{1,2},
A. Ortega-Moñux^{1,2}, J.G. Wangüemert-Pérez^{1,2}, Laura M. Lechuga⁴,
I. Molina-Fernández^{1,2}

¹ *E.T.S.I. Telecomunicación, Universidad de Málaga. Campus de Teatinos, 29071 Málaga, Spain*

² *Bionand Center for Nanomedicine and Biotechnology, P. Tecnológico de Andalucía, 29590 Málaga, Spain*

³ *Universidad de Oviedo, Departamento de Física, C/Federico García Lorca, 33007 Oviedo, Spain*

⁴ *Nanobiosensors and Bioanalytical Applications Group, Catalan Institute of Nanoscience and Nanotechnology (ICN2), CSIC, BIST and CIBER-BBN Campus UAB, 08193 Barcelona, Spain*

Tel: (+34) 952 13 13 11, Fax: (+34) 952 13 20 27, e-mail: imf@ic.uma.es

ABSTRACT

Silicon photonics enables sensitive and label-free optical biosensors for the detection of chemical and biological substances. Different sensing architectures have been used to improve the limit of detection and increase the dynamic range response. Here, we show experimental limit of detection at state-of-the-art level using silicon nitride integrated Mach-Zehnder interferometers with coherent read-out. These preliminary results are concordant with theoretical results, showing that the proposed approach enables the use of simple read-out equipment using low-cost laser sources.

Keywords: label-free biosensors, integrated optics, silicon photonics.

1. INTRODUCTION

Integrated photonic biosensors have been proposed to various applications such as food control, environmental safety, and clinical analysis. They can detect extremely-low quantities of specific analytes including proteins, DNA, and viruses [1]. Cheap manufacturing, small footprints and multiple detection are enabled due to CMOS fabrication compatibility [2]. Despite already demonstrating lab-on-chip (LOC) capabilities [3], i.e. performing different target detection in real-time and label-free, they are also candidates for future point-of-care (POC) devices [4, 5], which are light weight, small, cheap, and carriable equipment for the use at the treatment location.

Most photonic sensors rely on the penetration of the sensing mode into the bypassing analyte, meaning that the entering evanescent field is pushed or pulled in or out of the waveguides core thus modifying the modes propagating velocity, which can be detect using different approaches. Two ways of extracting this modification are resonant and interferometric sensing architectures. Even though resonant structures have comparable small footprints, interferometric architectures have demonstrated extreme limit of detections (LOD), down to 10^{-8} refractive index units (RIU) for homogeneous refractive index (HRI) changes of the ambient [6] and 100 fg/mm^2 for surface detection [5]. Resonant architectures often require a narrow linewidth tuneable optical source or a spectrum analysing device, whereas interferometric sensors do not demand such complex instruments. As both strategies rely of different reading systems, with different error sources, it has not been clear which alternative would offer better performance in terms of expected LOD. Recently a theoretical model has been presented which provides a common and simple theoretical framework in which the two architectures can be fairly compared [8].

The model is based on the use of a coherent reading technique [9] inherited from the field of optical communications [10] that circumvents some of the disadvantages of interferometric biosensors, such as sensitivity fading and directional ambiguity [1]. The model considers the optical losses and several noise sources of existing systems, making possible to compare the intrinsic LOD of interferometric and resonant sensors under the same levels of uncertainty (noise). Experimental results developed in our group [7] have shown the advantages of coherently detected interferometric sensing structures, demonstrating excellent detection limits of approximately 10^{-8} RIU when using a high-quality DFB top-bench laser source. Furthermore, very recent experiments confirm the theoretical model predictions that well balanced coherently detected interferometric biosensors are quite immune to noise sources coming from the laser source. This opens the possibility of using low cost and simple read-out techniques and low-cost laser sources.

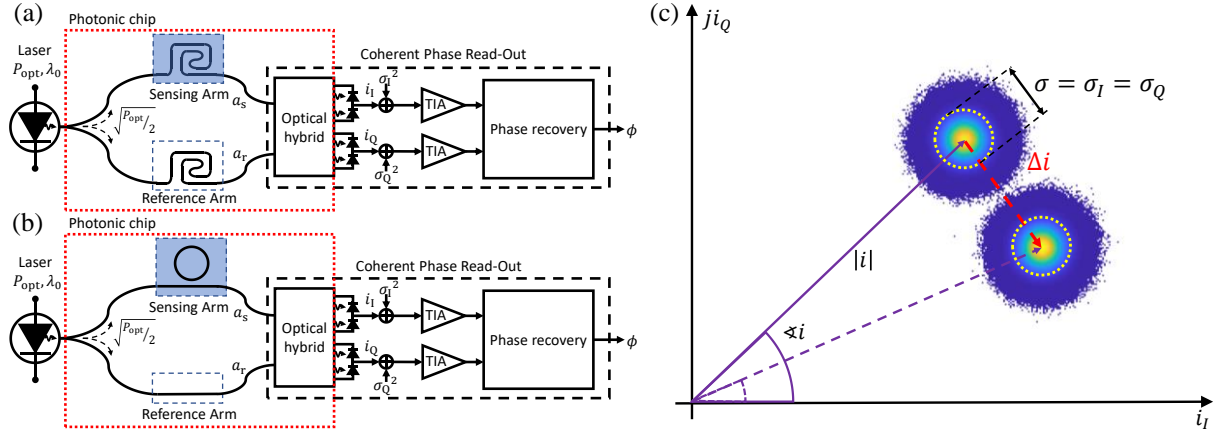


Figure 1. (a) MZI and (b) Ring resonator with coherent phase read-out. (c) Schematic representation of the coherently detected complex signal. The circle represents the noise (uncertainty) of the signal.

2. Theoretical Background

The theoretical model allowing direct comparison between interferometric and resonant silicon photonic biosensors is shown in Fig. 1(a), Fig 1(b)[8]. In this model, the laser source inputs optical power into a silicon sensor chip (dotted red line) comprising the reference and sensing arms (the sensing arm will be a spiral for interferometric and a resonant ring for resonant architectures, respectively) and an optical 90° hybrid (that can be easily achieved by a 2x4 MMI). Output light from the sensor chip is captured by external balanced photodiodes to get the real (\$i_1\$) and imaginary (\$i_Q\$) parts of the complex photocurrent = \$i_1 + j i_Q\$, from which the phase difference (\$\phi\$) between reference and sensing arms can be obtained. Theoretical analysis of the coherent detection process shows that the complex photocurrent can be easily calculated as \$i = R a_s a_r^*\$, where \$R\$ is the photodiode responsivity and \$a_r\$ and \$a_s\$ are the complex amplitudes of output signals from the reference and sensing arms, respectively. Detection uncertainty comes from white gaussian noise which is added to both real and imaginary channels with identical standard deviation \$\sigma = \sigma_I = \sigma_Q = \eta \sqrt{B}\$ with \$\eta\$ being the electrical noise spectral density and \$B\$ the systems bandwidth. Detection process in the complex plane is illustrated in Fig 1(c). In this figure, blue vectors show the complex photocurrents with and without analyte. The red vector \$\Delta i\$ shows the displacement of the complex photocurrent due to the presence of the analyte. The circles represent the region of uncertainty due to noise at the output of the photodetectors. The minimum detectable sensing index change \$\Delta n_s\$ can be calculated by \$|\Delta i| = |\partial i / \partial n_s \Delta n_s| = 3\sigma\$ which finally yields the LOD as \$LOD = 3\sigma / (|\partial i / \partial n_s| S_{\text{wg}})\$ where \$S_{\text{wg}}\$ is the waveguide sensibility.

2.1 Coherently Detected Mach-Zehnder Interferometer

For the Mach-Zehnder Interferometric (MZI) architecture, the complex envelopes at the output of the reference and sensing waveguides are respectively, \$a_r = \sqrt{P_{\text{opt}}/2} e^{j2\pi/\lambda_0 L n_r}\$ and \$a_s|_{\text{interf}} = \sqrt{P_{\text{opt}}/2} e^{-\alpha L} e^{j2\pi/\lambda_0 L n_s}\$, where \$P_{\text{opt}}\$ is the incoupling light power, \$\lambda_0\$ is the vacuum wavelength, \$\alpha\$ is the amplitude attenuation (in Np/m) due to absorption of the guided light in the buffer (no losses are considered in the reference waveguide which is buried in the low loss SiO₂ cladding) and \$n_r\$ and \$n_s\$ are, respectively, the refractive effective indexes of reference and sensing waveguide. Putting these equations into \$i = R a_s a_r^*\$, the limit of detection of interferometric architecture can be calculated as,

$$LOD_{\text{interf}} = \frac{3 \lambda_0 \eta \sqrt{B}}{\pi R P_{\text{opt}} S_{\text{wg}}} \frac{1}{L e^{\alpha L}}. \quad (1)$$

Figure 2(a) shows the detection limit of the interferometric case as a function of the sensing waveguides length \$L\$ with \$R = 1 \text{ A/W}\$, \$P_{\text{opt}} = 50 \mu\text{W}\$, \$\lambda_0 = 1.55 \mu\text{m}\$, \$S_{\text{wg}} = 0.8 \text{ RIU/RIU}\$, \$\alpha = 480 \text{ Np/m}\$, \$\eta = 3 \text{ pA/Hz}^{1/2}\$, \$B = 100 \text{ Hz}\$. It can be readily observed that the best LOD is achieved by setting \$L = 1/\alpha\$ yielding \$LOD_{\text{interf}} \approx 10^{-9} \text{ RIU}\$.

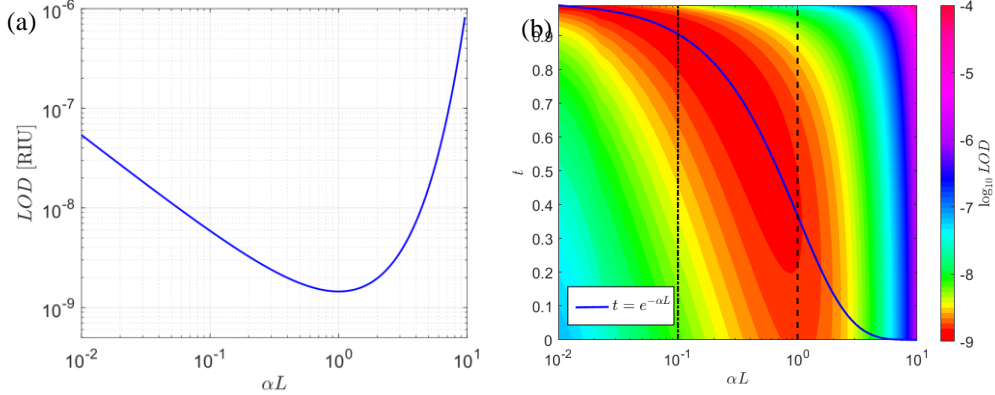


Figure 2. (a) Interferometric LOD as a function of the sensor length L . (b) The LOD of a coherently read ring resonator in logarithmic scale. The blue line represents the critical coupling condition.

2.2 Coherently Detected Ring Resonator

This simple system level point of view may also be applied to a ring resonator in a coherent detection scheme. Only a_s needs to be modified to $a_s|_{\text{res}} = \sqrt{P_{\text{opt}}/2} e^{-j\phi} (e^{-\alpha L} - te^{-j\phi}) / (1 - e^{-\alpha L} te^{-j\phi})$, with $\phi = 2\pi/\lambda_0 L n_s$, which is the common amplitude ring transfer function with t the transmission coefficient. As a result, the LOD for this case can be derived to,

$$\text{LOD}_{\text{res}} = \text{LOD}_{\text{interf}} \frac{|1 - te^{-\alpha L} e^{j\phi}|}{1 - t^2}. \quad (2)$$

Tuned to resonance, i.e. $\phi = 2\pi m$ with m a positive integer, eq. (2) is minimized for assuming critical coupling ($t = e^{-\alpha L}$) and $\alpha L \lesssim 1$, as demonstrated in Fig. 2(b). Therefore, the minimum detection limit achievable is $\text{LOD}_{\text{res}} \approx 1.9\alpha\lambda_0\eta\sqrt{B}/(S_{\text{wg}}RP_{\text{opt}})$, which is by a factor of 1.4 better than for the interferometric case. Worth highlighting is the case $t = 0$, for which eq. (2) simplifies to the interferometric case in eq. (1).

3. Experimental Work

3.1 Optimization

Based on the theoretical work done in [8], a more practical approach was realized in [7]. Figure 3a) shows the results of an optimization process performed on a photonic interferometric sensing setup with coherent read-out and a commonly used narrow linewidth (< 100 kHz) distributed feedback laser (DFB) with $\lambda_0 = 1.55$ μm . By identifying, for each step, the limiting noise source, e.g. sampling speed, mechanical vibrations, quantization-, and baseband noise, a reduction of overall seen noise was accomplished, such that a HRI limit of detection of approximately 10^{-8} RIU was obtained. The sensitivity of the silicon nitride waveguide is $S_{\text{wg}} \approx 0.22$ RIU/RIU, which is a comparatively poor waveguide sensitivity, demonstrating that ultra-sensitive limit of detection are still achievable without having optimized S_{wg} .

3.2 Narrow Linewidth vs. Fabry-Perot Laser with MZI

Coherently detected MZIs can be made insensitive to the noise caused by the optical source, i.e. relative intensity noise (RIN) and phase noise (PN) [8]. By the nature of the read-out, RIN will only affect the amplitude of the reconstructed signal. Furthermore, PN can be minimized by balancing both arms, i.e. $L n_s - L n_r \approx 0$. This implies that optical sources with extremely high linewidths should result in similar detection limits, as if a narrow linewidth source were used. For that purpose, a handheld Fabry-Perot (FP) and the DFB laser were used to perform a standard HRI calibration, injecting four different mass percentage solutions of sodium chloride (3%, 6%, 9%, 12%). The received optical power by the photodiodes is approximately -30 dBm for both cases. The corresponding phase shifts and the noise signals are shown in Fig. 3b). Sensitivities being similar, as expected, reveal that the LOD only is determined by the noise level, 1.2 mrad and 3.2 mrad for DFB and FP, respectively, resulting in 1.4×10^{-6} RIU and 5.2×10^{-7} RIU limit of detection in bulk, respectively. This experimental result indicates that lasers with high linewidths can indeed be used for biosensing purposes without significantly worsening the LOD if a balanced MZI with coherent read-out is used.

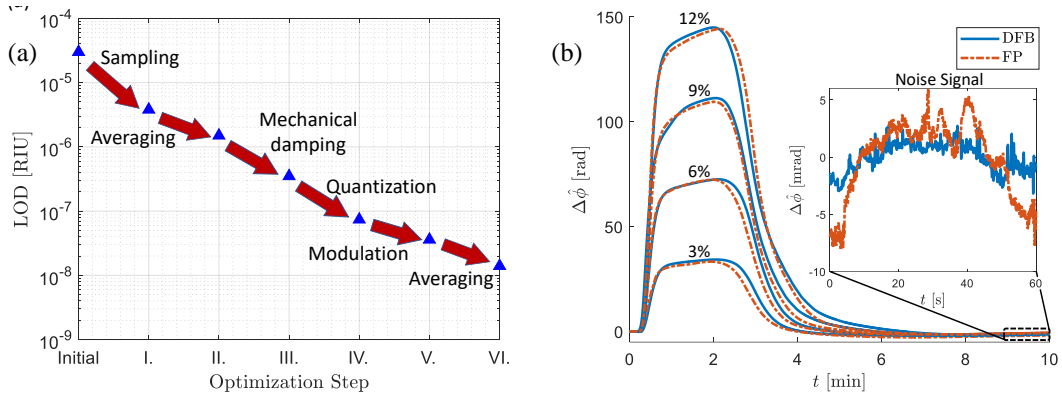


Figure 3. (a) Minimization of the LOD of a real MZI sensing system with coherent read-out due to different optimization steps different. (b) Phase response of the same system but with two different optical sources, a DFB and a Fabry-Perot (FP) laser.

4. CONCLUSIONS

A theoretical framework with coherent read-out has been presented, comparing the performance of resonant and interferometric sensing structures. Even though highly resonant sensors ($\alpha L \ll 1$) show a slightly better LOD, they are more prone to manufacturing imperfections, due to the strict critical coupling condition, than its interferometric counterpart. Additionally, they experience a higher wavelength dependency, thus being highly sensitive to PN. Hence the small performance gain does not justify the use of ring resonators in this context. Nevertheless, if the optimal length for interferometric sensors $\alpha L = 1$ cannot be reached by far, resonant structures with relaxed hardware requirements and less PN sensitivity, i.e. $0.1 < \alpha L < 1$ (see Fig. 2(b)), should be considered. Both types of sensors are theoretically immune to RIN, interferometric sensors regardless of the applied phase, and resonant structures only when tuned to resonance. Furthermore, we demonstrated that coherently detected balanced interferometric sensors are almost immune to laser PN in addition to their capacity to detect extremely small HRI changes while having poor waveguide sensitivity. Thus, optical sources with high linewidths can be used without severe performance losses.

ACKNOWLEDGEMENTS

European Union's Horizon 2020, Marie Skłodowska-Curie grant agreement No 713721. Ministerio de Economía y Competitividad (FEDER), Proyecto TEC2016-80718-R, and the Universidad de Málaga. Proyecto I+D+i, FEDER Andalucía 2014-2020 (UMA18-FEDERJA-219). ICN2 is supported by the Severo Ochoa program from Spanish MINECO (Grant No. SEV-2017-0706).

REFERENCES

- [1] A. Fernández Gavela, et al., "Last advances in silicon-based optical biosensors", *Sensors*, vol. 16, 285, (2016)
- [2] R. Baets, et al., "Silicon photonics: Silicon nitride versus silicon-on-insulator", *In Proceedings of the Optical Fiber Communication Conference*, Anaheim, CA, USA, pp. 1–3, 20–22, (2016)
- [3] M. Iqbal, et al., "Label-free biosensor arrays based on silicon ring resonators and high-speed optical scanning instrumentation," *IEEE J. Sel. Top. Quantum Electron.*, vol. 16, 3, pp. 654–661, (2010)
- [4] D. Martens, et al., "Study on the limit of detection in MZI-based biosensor systems," *Sci. Rep.*, vol. 9, no. 1, pp. 1–8, (2019)
- [5] A. B. González-Guerrero, et al., "Trends in photonic lab-on-chip interferometric biosensors for point-of-care diagnostics", *Anal. Methods*, vol. 8, 8380–8394, (2016)
- [6] R. J. van Gulik et al, "Refractive index sensing using a three-port interferometer and comparison with ring resonators", *IEEE J. Sel. Top. Quantum Electron.*, vol. 23, pp. 433–439, (2017)
- [7] J. Leuermann, et al., "Optimizing the limit of detection of waveguide-based interferometric biosensor devices", *Sensors*, vol. 19, 3671, (2019)
- [8] Í. Molina-Fernández, et al., "Fundamental limit of detection of photonic biosensors with coherent phase read-out", *Opt. Express*, vol 27, pp. 12616-12629, (2019)
- [9] R. Halir, et al, "Direct and sensitive phase readout for integrated waveguide sensors", *IEEE Photon. J.*, vol. 5, 6800906, (2013)
- [10] P. J. Reyes-Iglesias, et al., "High-performance monolithically integrated 120° downconverter with relaxed hardware constraints", *Opt. Express*, vol. 20, pp. 5725-5741, (2012)